Vision, Modeling, and Visualization (2011)
Peter Eisert, Konrad Polthier, and Joachim Hornegger (Eds.)

Measuring BRDFs of immersed materials

Kai Berger[†], Ilya Reshetouski[‡], Marcus Magnor[§] & Ivo Ihrke[¶]

Abstract

We investigate the effect of immersing real-world materials into media of different refractive indices. We show, that only some materials follow the Fresnel-governed behaviour. In reality, many materials exhibit unexpected effects such as stronger localized highlights or a significant increase in the glossy reflection due to microgeometry. In this paper, we propose a new measurement technique that allows for measuring the BRDFs of materials that are immersed into different media.

1. Introduction

A familiar effect in everyday life is that objects change their appearance when immersed in water or other substances with refractive indices different from air. Some common examples include diffusers that lose their diffusing characteristics when coated e.g. with oil, becoming more transparent in the process. Another effect is the subtly different appearance of objects underwater that are observed, e.g., during diving: Picking up an object observed under water and observing it on the beach when dry will usually result in quite a different look.

This *refractive index dependence* of bidirectional scattering distribution functions (BSDFs) has so far been mostly ignored. Implicitly it is assumed to be governed by the Fresnel equations via the refractive index dependence of the Fresnel reflection and transmission factors, as are used in most physics-based BRDF models [TS67, CT81, HTSG91, APS00]. An exception is the BRDF model for finished wood by Marschner et al. [MWAM05]. Here, however, the focus is on the refractive properties of the surface finishing. The surrounding medium is still assumed to be air.

In this paper we measure the reflectance properties of a range of materials in the presence of a refractive immersing medium such as water or salt solutions.

We present a measurement apparatus to measure BSDFs in different refractive media and acquire a database of a wide range of representative materials.

The paper is structured as follows: After revisiting the related work in the field of BRDF capturing and modeling in Section 2, we give a short overview about specular reflection and refraction at material boundaries in Section 3. We show that the Fresnel term is the governing factor for the surface appearance of materials placed into different media. We then introduce our measurement setup in Section 4 to measure the BRDFs of immersed materials.

2. Related Work

Phenomenological Models are based on an intuitive modeling of the reflection process such as the famous Phong model [Pho75]. Usually, purely ad-hoc methods such as the original Phong model, and *physically plausible* BRDF models fall into this category where the latter characterization refers to the fact that ad-hoc models can be built such that they do not obviously violate the principles of positivity, reciprocity, and energy conservation.

Physics-Based Models originated in the optics literature. The seminal work of Torrance and Sparrow [TS67] was introduced to computer graphics by Blinn [Bli77]. Cook and Torrance [CT81] extended the micro-facet model to use Beckmann's [BS63] micro-facet distribution function. Kajiya [Kaj85] developed a micro-facet model for anisotropic rough surfaces, based on an integral description using wave optics. He tabulated the BRDF values for efficient computation.

Measurement-Based Models take a different approach. Instead of creating models from analytical descriptions of

† TU Braunschweig e-mail: berger@cg.cs.tu-bs.de
‡ MMCI Saarbruecken e-mail: iresheto@mmci.uni-saarland.de
§ TU Braunschweig e-mail: magnor@cg.cs.tu-bs.de
¶ MMCI Saarbruecken e-mail: ihrke@mmci.uni-saarland.de

DOI: 10.2312/PE/VMV/VMV11/325-330

physical processes, they are based on measurements of the reflection properties of real-world materials. Suitable functions that describe the observed behavior are then fitted while preserving the basic BRDF properties as in the phenomenological models. Examples of this approach are the anisotropic Ward model [War92]. He et al. [HTSG91] also show fits of their physics-based model to real-world data. The Lafortune model [LFTG97] was specifically developed to fit observed data well. A different approach is taken by Matusik et al. [MPBM03a]. The authors acquire a large data base of reflectance data for a wide range of materials. They then analyze the data using PCA and nonlinear dimensionality reduction techniques [Bra03] to derive a low-parametric model given the initial data. Kautz et al. [KM99] present a method that uses spherical harmonics as representation for the captured data.

BRDF Acquisition has been performed using a variety of devices. The most commonly used tool in optics is the gonioreflectometer, where a planar sample is analyzed by a hemispherical adjustable detector and light source. Marschner et al. [MWLT00] developed an image-based BRDF measurement technique based on spherical samples. This way, moving the detector can be avoided and BRDFs with a high resolution in the viewing direction can be acquired. This technique is the prevailing technique for BRDF acquisition in graphics. Matusik et al. [MPBM03c] use a similar setup but propose to reduce the number of measurements by using their data base [MPBM03a]. An evaluation of analytical BRDF models for data fitting purposes has been performed by Ngan et al. [NDM05]. Ghosh et al. [GHAO08] expand the BRDF measurements in an optical basis and directly measure the basis coefficients, removing the need for any mechanical parts. Recently, Hullin et al. [HHA*10] have extended the concept of a monochromatic BRDF to account for bi-spectral interaction, i.e. conversion of the wavelength of light by the material as e.g. in fluorescent materials. They do not develop a model based on their measured data.

Methods for acquiring spatially varying BRDFs have also been developed [Dan01, LKG*03, MMS*05] but are of less interest in the context of the proposed method.

BTDF

The bidirectional transmittance distribution function (BTDF) models describe the transmission of light at the boundary of materials. While Dai et al. [DWL*09] and Walter et al. [WMLT07] present BTDF models for the entire entrance and exit process of light, the following papers present BTDFs for subsurface effects of opaque materials. Weidlich et al. [WW07] describe a multi-layer model for rendering of metallic paints or frosted metal and Hanrahan et al. [HK93] describe a layered surface model for subsurface reflectance that takes the Fresnel effect into account. The interaction of water with surfaces has been adressed by some papers beforehand. Lu et al. [LGR*05] describe the geometry-based drying process of objects spilled with water and Sun et al. [SSR*07] describe time-varying BRDFS (TV-BRDFs), for example dust accumulation and the drying of spray and oil paint. Gu et al. [GRBN07] describe a thin-layer BTDF model for rendering dirty and contaminated glass.

All previously presented methods do not account for intensity changes of reflected light for submerged surfaces. Our work addresses this gap by introducing a new measurement setup for capturing BRDFs of different materials that are placed into media with different refractive index.

3. Background

Specular reflection and refraction at material boundaries is caused by a change of the electric and magnetic fields across the interface. The exact description of the effect requires electromagnetic wave optics, i.e., solutions must satisfy Maxwell's equations. In graphics, however, geometric optics is the dominant model for describing and simulating the effects of light's interaction with matter. The basic tool for describing general reflections in graphics is the bidirectional reflectance distribution function (BRDF), and similarly, the bidirectional transmittance distribution function (BTDF) for refracted rays. Together these two functions are known as bidirectional scattering distribution function (BSDF). The BSDF can be considered the mean reflectance and transmittance of a material due to micro-scale global illumination effects at material structures much smaller than the incident beam spot size.

Physics-based BRDF models, which are often used to also describe BTDF's [WMLT08], are based on analytical derivations which are usually based on a specific surface micro-geometry and reflection model. Most commonly, perfectly mirroring micro-facets, so called Fresnel reflectors, are assumed as the basic building blocks of the micro-geometry [TS67, CT81, HTSG91, APS00, MWAM05].

Fresnel Reflection and Transmission are the main factors in these models that influence non-diffuse surface appearance. They are generally of the form [HTSG91]:

$$f_r = \lambda_s \rho_s + \lambda_{dd} \rho_{dd} + \lambda_{ud} \rho_{ud}, \tag{1}$$

where λ_s, λ_{dd} and λ_{ud} are the color multiplicative factors and ρ_s denotes perfect specular reflectance, ρ_{dd} directionally diffuse reflectance, ρ_{ud} perfect Lambertian reflectance, and f_r is the resulting BRDF. The specular and directionally diffuse terms are influenced by Fresnel reflection which enters the equation as a multiplicative factor

$$\rho_s = F_r \cdot L_i \tag{2}$$

$$\rho_{dd} = F_r \cdot D \cdot S, \tag{3}$$

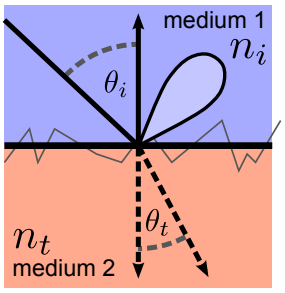

Figure 1: *Geometry for micro-facet BRDF models. An incident ray makes an angle θ_i with the surface normal. The surface is assumed to be a flat interface, representing the mean of the surface micro-geometry (grey). The interface is separating two media with refractive indices n_i and n_t, respectively. Observe that opaque materials also have refractive indices, e.g. plastic has an index of ≈ 1.46. The Fresnel equations determine the amount of reflected and transmitted light. The lobe of the BRDF is indicated in light blue.*

where L_i is the incident radiance, D is the statistical micro-facet distribution, S is the shadowing term, and F_r is the Fresnel reflection coefficient. In the following, we assume unpolarized light as this is the most common situation in computer graphics. The Fresnel reflection coefficient F_r is then given by

$$F_r = \frac{1}{2}\left(r_\perp^2 + r_\parallel^2\right) \quad (4)$$

$$r_\perp = \frac{(n_i \cos\theta_i - n_t \cos\theta_t)}{(n_i \cos\theta_i + n_t \cos\theta_t)} \quad (5)$$

$$r_\parallel = \frac{(n_t \cos\theta_i - n_i \cos\theta_t)}{(n_t \cos\theta_i + n_i \cos\theta_t)}, \quad (6)$$

see Fig. 1. Note that the Fresnel reflection coeffecient is governed by the factors n_i, the refractive index of the surrounding medium, and n_t, the refractive index of the material. Both factors will be crucial for examining the effects that we measured. Due to energy conservation, the transmitted light is the light that is not being reflected off the surface and thus the Fresnel transmission coefficient is $F_t = 1 - F_r$.

Physics-Based BRDF Models assume that Fresnel reflection is the only process that is influenced by refractive index changes of the surrounding medium [TS67, CT81, HTSG91, APS00, MWAM05].

We show that current physics-based BRDF models do not adequately represent the refractive index dependence of the reflectance observed in reality. According to specular micro-facet BRDF models, the Fresnel effect is the dominant source of change in the shape of the reflectance lobes. For essentially diffuse objects, the Oren-Nayar [ON94] model predicts a constant BRDF.

θ_i^r, θ_o^r	incoming and outgoing angle w.r.t. normal for reflection at sample
θ_i^t, θ_o^t	incoming and outgoing angle w.r.t. normal for transmission at screen
ω_i^r, ω_o^r	incoming and outgoing angle for reflection at sample
ω_i^t, ω_o^t	incoming and outgoing angle for transmission at screen
f_r	BRDF of sample
f_t	BTDF of screen
$\Delta\omega_i^r$	solid angle subtended by laser as seen from sample
$\Delta\omega_i^t$	solid angle subtended by laser spot on sample as seen from screen
L_i^r	radiance incident on sample (from laser)
$L_o^r = L_i^t$	radiance exitant from sample (and incident on screen)
$L_o^t = L_c$	radiance exitant from screen (and recorded by camera)

(a) Table of symbols

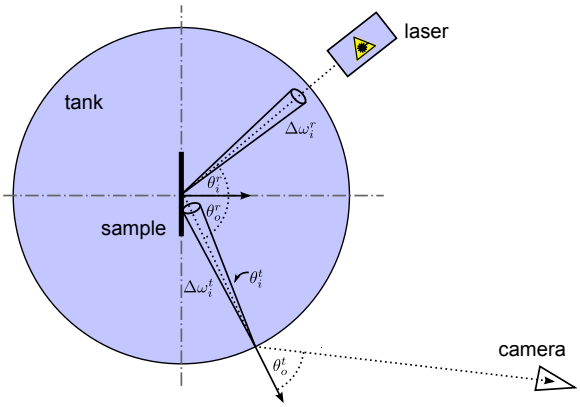

(b) BTDF calibration

Figure 2: *The table of symbols used in the paper and the geometric layout for BTDF calibration*

We analyze the dependence of material reflectance properties on the refractive index of the surrounding medium. We present a measurement apparatus to measure isotropic refractive index-dependent bidirectional scattering distribution functions. We record a database of representative materials to verify the reflectance properties under refractive index changes.

Furthermore, we propose a method to measure the refractive index dependent BSDF and simultaneously determine the refractive index of the material sample.

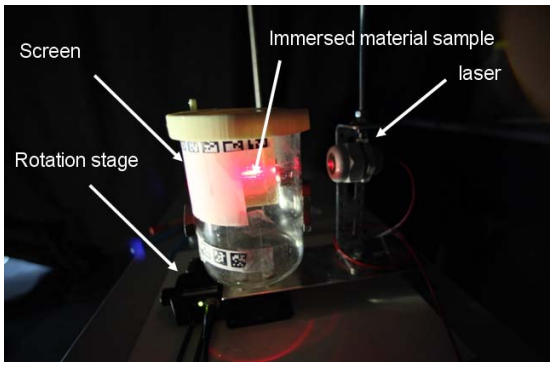

Figure 3: *Our measurement setup: a material patch is placed in the diameter of the cylinder. The cylinder is filled with the surrounding medium. A rotating laser then shines in the range of* 0° *to* 90°*. The reflected light is imaged by a screen, which is attached to the cylinder and captured by a CCD camera.*

4. BRDF Measurements

4.1. Measurement Setup

For the purpose of our experiment, we developed a new measurement setup. This setup allows to measure the BRDF of submerged materials. To our knowledge, existing devices are not suitable for acquiring reflectance data for samples immersed in a refractive medium.

Our setup is shown in Fig. 3. The material sample is immersed in a medium with a refractive index different from air. The cylinder contains the medium and the sample. A laser, mounted on a rotation stage, illuminates the sample from different angles. The laser ray hits the cylinder wall orthogonally for all acquisition angles, eliminating refraction upon entry into the medium, which would occur otherwise. A screen is attached directly to the cylinder wall in order to minimize the refraction on the exitant light path. The screen is imaged by a CCD camera (not shown), recording a slice of the sample BRDF attenuated by the BTDF of the screen.

To calibrate our system, we first compute the geometry of the setup using fiducial markers attached to the cylinder [SSS06]. We then proceed to calibrate the BTDF of the screen by recording a *calibration sample*. We use Labsphere Spectralon for this purpose [VZ06]. This material exhibits almost perfect Lambertian reflectance and a high albedo of $\approx 99\%$ for a wide range of wavelengths including the visible spectrum. To acquire the BTDF of the measurement screen we perform an image-based measurement that is valid for the geometric calibration determined previously.

First, we discuss the image formation in our BSDF measurement device. We refer to Fig. 2 for a description of the symbols used in the following. The radiance reflected from the sample is given by

$$L_o^r(\omega_o^r) = L_i^r(\omega_i^r) f_r(\omega_i^r, \omega_o^r) \cos\theta_i^r \Delta\omega_i^r. \tag{7}$$

We assume that L_i^r is approximately constant as opposed to Gaussian over $\Delta\omega_i^r$, therefore the integration is reduced to a simple multiplication. We will see that this assumption does not affect our calibration procedure. Similarly, the radiance registered by the camera is

$$L_c = L_o^t(\omega_o^t) = L_i^t(\omega_i^t) f_t(\omega_i^t, \omega_o^t) \cos\theta_i^t \Delta\omega_i^t, \tag{8}$$

and, as in the previous case, we assume $L_i^t(\omega_i^t)$ to be constant over $\Delta\omega_i^t$. This is only an approximation since the laser spot usually exhibits a Gaussian profile. Note, that $\Delta\omega_i^r$ varies as with $\cos\omega_i$ due to projected area foreshortening. Setting $\Delta\omega_i^t = \cos\theta_o^r \cdot c_0$, the cosine times some diffuse constant c_0 and combining Eqs. 7 and 8, we obtain

$$L_c = L_i^r(\omega_i^r) f_t(\omega_i^t, \omega_o^t) f_r(\omega_i^r, \omega_o^r) \cos\theta_i^t \cos\theta_o^t \cos\theta_i^r c_0. \tag{9}$$

This equation describes the recorded radiance due to a sample illuminated by a laser from direction ω_i^r.

Now, we perform a measurement with the *calibration sample*. We thus obtain a reference measurement

$$L_c^{Spectralon} = L_i^r(\omega_i^r) f_t(\omega_i^t, \omega_o^t) \frac{1}{\rho} \cos\theta_i^t \cos\theta_o^t \cos\theta_i^r c_0, \tag{10}$$

where $\frac{1}{\rho} \approx 0.99 \cdot \frac{1}{4\pi}$ is the BRDF of Spectralon. Now, taking an arbitrary BRDF measurement, Eq. 9, and dividing by the Spectralon reference measurement, Eq. 10, the geometric terms cancel and we obtain

$$f_r = \rho \cdot \frac{L_c}{L_c^{Spectralon}}, \tag{11}$$

i.e. we can directly measure a value proportional to the BRDF of the sample. Since we are recording a full slice of the BRDF for every incident angle of the laser, we perform the calibration for every laser angle. This is not strictly necessary since the diffuse BRDF of Spectralon does not vary with the incident angle. However, since our laser beam is only approximately centered we ensure a proper measurement this way. Note, that the diffuse constant c_0 has to be fitted to the measured data, e.g. with a suitable BRDF model.

Processing

Each incident angle is imaged with different exposure times $(\frac{1}{4000}s, \frac{1}{1000}s, \frac{1}{250}s, \frac{1}{60}s, \frac{1}{25}s, \frac{1}{4}s, 1s)$ to account for the dynamic range of the reflected laser light. The resulting images

Figure 4: *Backprojection of the captured images onto the surface of a parametrized cylinder. The captured specular highlight (red) matches the predicted reflection point ($\theta_o = \theta_i$, yellow).*

for each incident angle are backprojected [Eve01] onto the surface of a cylinder which is fitted with RANSAC to the reconstructed geometry of the setup, 4. Then, the backprojected images are combined to one HDR-image [MKMS07] which is then downsampled to size 249×180 px and stored according to the corresponding incident angle.

5. Results

We captured the following classes of materials: Acrylic paint, aluminum, bamboo, ceramics, cloth, oil paint, plastic, sandpaper, stone, Teflon and wood. We found that only bamboo and plastic show significantly different reflectance behaviour for different media. The other materials did not show a different reflectance behaviour for different refractive indices, Fig. 5. To render our results we loaded the measured BRDF-data in the MERL-file format [MPBM03b] and rendered a scene in PBRT [PH04]. The rendering time took approximately 10 minutes per frame on a 2.2 Ghz Intel Core 2Duo processor with a NVIDIA GeForce G210M graphics card, the image resolution was 768×576 pixel, Fig. 6.

6. Conclusion

We have investigated the effect of immersing a material into different media and compared the measured behavior with the prediction of the Fresnel term. We presented a new method to measure the material behaviour by placing it at the center of a cylinder and imaging the reflected laser light with a screen attached to the cylinder. The measured data were used for rendering virtual scenes of objects immersed into water. We figure, the main applications of the capturing setup is the provide data for realistic underwater renderings or renderings of plastic materials exposed to liquids. In the future we want to extend the measurement setup to account for anisotropic materials and retroreflectance. Furthermore we want to investigate the effect with submerged multi-layer materials.

Acknowledgements

This work has been funded by the German Science Foundation, DFG MA2555/5-1. This work was funded by the German Research Foundation (DFG) within the Cluster of Excellence Multimodal Computing and Interaction.

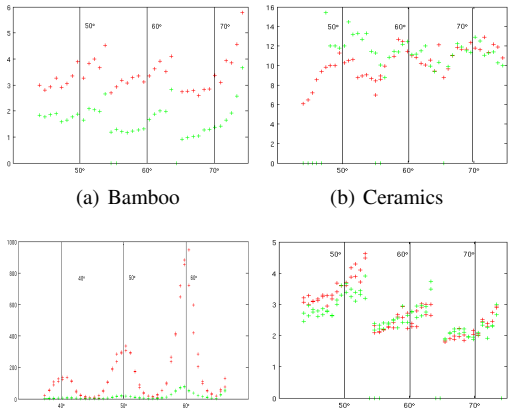

(a) Bamboo (b) Ceramics

(c) Red Plastic (d) Stone

Figure 5: *The differences in measured reflectance for refractive indices 1.0 (red) and 1.44 (green) of the surrounding medium for different materials. While Ceramics and Stone do not show significant differences, Bamboo and Red Plastic are clearly distinguishable. The exitant reflectance is measured for $\phi_o = 0^\circ$ and $\theta_o \in [45^\circ, 75^\circ]$ for incident angles 50°,60° and 70° w.r.t. the surface normal. The vertical lines denote $\theta_o = \theta_i$ for each incident angle.*

(a) Bamboo (b) Red Plastic

Figure 6: *The effects of different surrounding media to the size of the specular reflection in the proposed model: In each image, the left side of the model shows the reflection of the material for air (≈ 1.0) and the right side shows for water with refractive index ≈ 1.33. The small boxes show a close-up view to the particular highlight. Note, that the intensity and the extent of the highlight decreases with increasing refractive index for both materials. Black spots correspond to input angles outside the measured range*

References

[APS00] ASHIKMIN M., PREMOŽE S., SHIRLEY P.: A Micro-Facet Based BRDF Generator. In *Proc. of SIGGRAPH* (2000), pp. 65–74. 1, 2, 3

[Bli77] BLINN J. F.: Models of Light Reflection for Computer Synthesized Pictures. In *Proc. of SIGGRAPH* (1977), pp. 192–198. 1

[Bra03] BRAND M.: Charting a Manifold. *NIPS 15* (2003), 985–992. 2

[BS63] BECKMANN P., SPIZZICHINO A.: *The Scattering of Electromagnetic Waves from Rough Surfaces*. Pergamon Press, 1963. 1

[CT81] COOK R. L., TORRANCE K. E.: A Reflectance Model for Computer Graphics. In *Proc. of SIGGRAPH* (1981), pp. 307–316. 1, 2, 3

[Dan01] DANA K. J.: BRDF/BTF Measurement Device. In *Proc. of ICCV* (2001), pp. 265–272. 2

[DWL*09] DAI Q., WANG J., LIU Y., SNYDER J., WU E., GUO B.: The Dual-microfacet Model for Capturing Thin Transparent Slabs. *CGF 28*, 7 (2009), 1917–1925. 2

[Eve01] EVERITT C.: Projective texture mapping. *White paper, NVidia Corporation* (2001). 4

[GHAO08] GHOSH A., HEIDRICH W., ACHUTHA S., O'TOOLE M.: A Basis Illumination Approach to BRDF Measurement. *IJCV* (2008). 2

[GRBN07] GU J., RAMAMOORTHI R., BELHUMEUR P., NAYAR S. K.: Dirty Glass: Rendering Contamination on Transparent Surfaces. In *Proc. of EGSR* (2007), pp. 159–170. 2

[HHA*10] HULLIN M. B., HANIKA J., AJDIN B., KAUTZ J., SEIDEL H.-P., LENSCH H. P. A.: Acquisition and Analysis of Bispectral BRDFs. *Trans. Graph. 29*, 3 (2010), to appear. 2

[HK93] HANRAHAN P., KRUEGER W.: Reflection from Layered Surfaces due to Subsurface Scattering. In *Proc. of SIGGRAPH* (1993), pp. 164–174. 2

[HTSG91] HE X. D., TORRANCE K. E., SILLION F. X., GREENBERG D. P.: A Comprehensive Physical Model for Light Reflection. In *Proc. of SIGGRAPH* (1991), pp. 175–186. 1, 2, 3

[Kaj85] KAJIYA J. T.: Anisotropic Reflection Models. In *Proc. of SIGGRAPH* (1985), pp. 15–21. 1

[KM99] KAUTZ J., MCCOOL M.: Interactive rendering with arbitrary BRDFs using separable approximations. In *Eurographics Rendering Workshop 1999* (1999), vol. 18, Citeseer. 2

[LFTG97] LAFORTUNE E. P. F., FOO S.-C., TORRANCE K. E., GREENBERG D. P.: Non-linear Approximation of Reflectance Functions. In *Proc. of SIGGRAPH* (1997), pp. 117–126. 2

[LGR*05] LU J., GEORGHIADES A. S., RUSHMEIER H., DORSEY J., XU C.: Synthesis of Material Drying History: Phenomenon Modeling, Transferring and Rendering . In *Proc. of Workshop on Natural Phenomena* (2005), pp. 175–184. 2

[LKG*03] LENSCH H. P. A., KAUTZ J., GOESELE M., HEIDRICH W., SEIDEL H.-P.: Image-based Reconstruction of Spatial Appearance and Geometric Detail. *Transactions on Graphics 22*, 2 (2003), 234–257. 2

[MKMS07] MANTIUK R., KRAWCZYK G., MANTIUK R., SEIDEL H.-P.: High dynamic range imaging pipeline: Perception-motivated representation of visual content. In *Human Vision and Electronic Imaging XII* (San Jose, USA, February 2007), Rogowitz B. E., Pappas T. N., Daly S. J., (Eds.), vol. 6492 of *Proceedings of SPIE*, SPIE. 4

[MMS*05] MÜLLER G., MESETH J., SATTLER M., SARLETTE R., KLEIN R.: Acquisition, Synthesis and Rendering of Bidirectional Texture Functions. *CGF 24*, 1 (2005), 83–109. 2

[MPBM03a] MATUSIK W., PFISTER H., BRAND M., MCMILLAN L.: A Data-Driven Reflectance Model. *Transactions on Graphics 22*, 3 (2003), 759–769. 2

[MPBM03b] MATUSIK W., PFISTER H., BRAND M., MCMILLAN L.: A data-driven reflectance model. *ACM Transactions on Graphics 22*, 3 (July 2003), 759–769. 5

[MPBM03c] MATUSIK W., PFISTER H., BRAND M., MCMILLAN L.: Efficient Isotropic BRDF Measurement. In *Proc. of EGSR* (2003), pp. 241–247. 2

[MWAM05] MARSCHNER S. R., WESTIN S. H., ARBREE A., MOON J. T.: Measuring and Modeling the Appearance of Finished Wood. *Trans. Graph. 24*, 3 (2005), 727–734. 1, 2, 3

[MWLT00] MARSCHNER S. R., WESTIN S. H., LAFORTUNE E. P. F., TORRANCE K. E.: Image-based Bidirectional Reflectance Distribution Function Measurement. *Applied Optics 39*, 16 (2000), 460–466. 2

[NDM05] NGAN A., DURAND F., MATUSIK W.: Experimental Analysis of BRDF Models. In *Proc. of EGSR* (2005), pp. 117–126. 2

[ON94] OREN M., NAYAR S. K.: Generalization of Lambert's Reflectance Model. In *Proc. of SIGGRAPH* (1994), pp. 239–246. 3

[PH04] PHARR M., HUMPHREYS G.: *Physically based rendering: From theory to implementation*. Morgan Kaufmann, 2004. 5

[Pho75] PHONG B. T.: Illumination for Computer Generated Pictures. *Comm. ACM 18*, 6 (1975), 311–317. 1

[SSR*07] SUN B., SUNKAVALLI K., RAMAMOORTHI R., BELHUMEUR P. N., NAYAR S. K.: Time-Varying BRDFs. *TVCG 13*, 3 (2007), 595–609. 2

[SSS06] SNAVELY N., SEITZ S., SZELISKI R.: Photo Tourism: Exploring image collections in 3D. *ACM Transactions on Graphics (Proceedings of SIGGRAPH 2006)* (2006). 4

[TS67] TORRANCE K. E., SPARROW E. M.: Theory for Off-Specular Reflection from Roughened Surfaces. *JOSA 57*, 9 (1967), 1105–1114. 1, 2, 3

[VZ06] VOSS K. J., ZHANG H.: Bidirectional Reflectance of Dry and Submerged Labsphere Spectralon Plaque. *Applied Optics 45*, 30 (2006), 7924–7927. 4

[War92] WARD G. J.: Measuring and Modeling Anisotropic Reflection. In *Proc. of SIGGRAPH* (1992), pp. 265–272. 2

[WMLT07] WALTER B., MARSCHNER S. R., LI H., TORRANCE K. E.: Microfacet Models for Refraction through Rough Surfaces . In *Proc. of EGSR* (2007), pp. 195–206. 2

[WMLT08] WALTER B., MARSCHNER S., LI H., TORRANCE K.: Eurographics Symposium on Rendering (2007) Jan Kautz and Sumanta Pattanaik (Editors) Microfacet Models for Refraction through Rough Surfaces. 2

[WW07] WEIDLICH A., WILKIE A.: Arbitrarily Layered Micro-Facet Surfaces. In *Proc. of Pacific Graphics* (2007), pp. 171–178. 2